Princeton Plasma Physics Laboratory

PPPL-4063 **PPPL-4063**

Plasma Shape Control on the National Spherical Torus Experiment using Real-time Equilibrium Reconstruction

D.A. Gates, J.R. Ferron, M. Bell, T. Gibney, R. Johnson,
R.J. Marsala, D. Mastrovito, J.E. Menard, D. Mueller,
B. Penaflor, S.A. Sabbagh, and T. Stevenson

April 2005

Prepared for the U.S. Department of Energy under Contract DE-AC02-76CH03073.

PPPL Report Availability

This report is posted on the U.S. Department of Energy's Princeton Plasma Physics Laboratory Publications and Reports web site in Fiscal Year 2005. The home page for PPPL Reports and Publications is: http://www.pppl.gov/pub_report/

Office of Scientific and Technical Information (OSTI):

Available electronically at: http://www.osti.gov/bridge.

Available for a processing fee to U.S. Department of Energy and its contractors, in paper from:

U.S. Department of Energy
Office of Scientific and Technical Information
P.O. Box 62
Oak Ridge, TN 37831-0062

Telephone: (865) 576-8401

Fax: (865) 576-5728

E-mail: reports@adonis.osti.gov

National Technical Information Service (NTIS):

This report is available for sale to the general public from:

U.S. Department of Commerce
National Technical Information Service
5285 Port Royal Road
Springfield, VA 22161

Telephone: (800) 553-6847

Fax: (703) 605-6900

Email: orders@ntis.fedworld.gov

Online ordering: http://www.ntis.gov/ordering.htm

Plasma shape control on the National Spherical Torus Experiment (NSTX) using real-time equilibrium reconstruction

D. A. Gates[1], J. R. Ferron[2], M. Bell[1], T. Gibney[1],

R. Johnson[2], R. J. Marsala[1], D. Mastrovito[1], J. E. Menard[1],

D. Mueller[1], B. Penaflor[2], S. A. Sabbagh[3], T. Stevenson[1]

[1]*Plasma Physics Laboratory, Princeton University, P.O.Box 451, Princeton, New Jersey 08543*

[2]*General Atomics, La Jolla, California 92186*

[3]*Columbia University, New York, New York 10027*

Abstract

Plasma shape control using real-time equilibrium reconstruction has been implemented on the National Spherical Torus Experiment. The rtEFIT code originally developed for use on DIII-D was adapted for use on NSTX. The real-time equilibria provide calculations of the flux at points on the plasma boundary, which is used as input to a shape control algorithm known as isoflux control. The flux at the desired boundary location is compared to a reference flux value, and this flux error is used as the basic feedback quantity for the poloidal field coils on NSTX. The hardware that comprises the control system is described, as well as the software infrastructure. Examples of precise boundary control are also presented.

1 Introduction

Tokamak position control was first implemented (see, e.g reference [1]) in the second generation of tokamak devices, i.e. those that employed an externally applied vertical field rather than a copper shell to maintain toroidal equilibrium. These early systems consisted of strategically placed magnetic pick-up coils connected to analog circuits which drove the vertical field power supplies. Since that time the field of tokamak plasma boundary control has matured substantially through several distinct phases; first to produce elongated plasmas that required vertical stabilization, and then to more complex shapes (D-shaped plasmas, bean shaped plasmas, etc.). As shapes became more complex, so did control schemes. There are literally hundreds of published works which have as their primary topic the control of the tokamak plasma boundary. Recently, computers have advanced to the point where inverting the Grad-Shafranov equation [2, 3] is possible on a timescale that is useful for controlling the plasma discharge. This capability has moved the field of plasma boundary control out of the realm of electrical engineering into the realm of plasma physics, since realistic solutions to the plasma force balance can be used as inputs to feedback loops.

The rtEFIT code [4] has recently been implemented on a low aspect ratio device - the National Spherical Torus Experiment. The isoflux control [5] algorithm was also imported for use on NSTX. This paper will describe, in Section 2, the computer hardware that is presently in use for control on NSTX and that is used for the real-time reconstructions. The associated real-time communication hardware will also be described. In addition, in Section 3, the software infrastructure that has been adopted will be outlined. Section 4 describes the control software currently in use on NSTX, including: 1) a simple algorithm that was used for the first several NSTX physics campaigns, and which is still in use during the early current ramp preceding rtEFIT control, and 2) a brief description of the rtEFIT/isoflux system with emphasis on the aspects unique to NSTX. With this background, plasma control using the rtEFIT/isoflux control system will be described in Section 5.

2 Hardware

The NSTX plasma control system computer consists of 8 333MHz processors in a shared memory architecture. The processor cards are built by Sky Computers (Helmsford, MA). Each processor motherboard contains 4 G4 processors (Motorola) and one Front Panel Data Port (FPDP - ANSI/VITA

17) high speed low-latency direct memory access i/o port. The two mother boards are connected together by a VME P2 backplane known as “Skychannel” (ANSI/VITA 10-1995). The real-time computer is not available for interactive processes, but is instead accessed over the VME backplane from a single-board workstation built by Force Computers (Fremont, CA). The Force computer runs the Solaris operating system written by SUN computers (Stanford, CA) and also acts as the VME Slot 0 controller.

Data is acquired in real-time at 5kHz over a distributed network of point-to-point connections from VME crates that contain one or more 9421 (12bit) or 9422 (16bit) FPDP digitizers (Merlin Electronics, Memphis, TN). There are currently 192 channels of data being acquired in four different locations. The data consists of magnetic field and flux measurements, power supply currents and voltages for shape control. Gas control data and current, voltage, and phase data for the antenna elements of the RF heating system [6] are also acquired in real time, but are not yet used in the shape control system. The distributed data acquisition system is required due to the rather complex grounding scheme on NSTX needed for the coaxial helicity injection system [7] which biases a large fraction of the NSTX vacuum vessel to $\sim$ 1kV potentials.

The data is transmitted over a fiber optic serial link known as Serial FPDP (ANSI/VITA 17.1-2003) built by Systran Corporation (Dayton, OH). The independent point-to point data streams are multi-plexed into a single data stream by a module known as FIMM (or FPDP Input Multiplexing Module, developed at PPPL) which does a simple concatenation of the individual streams into a single stream after FIFO (First-In-First-Out) buffering. The data is then streamed into the FPDP port on the first computer board. The measured end-to-end latency of the data acquisition system is $4\mu s$.

Power supply commands are issued through the second FPDP i/o card to a module developed at PPPL known as a PCLIM (PC-Link Interface Module) which converts data into the digital format of the PCLink (Power Conversion Link) which was developed for use on TFTR (Tokamak Fusion Test Reactor) in the early 1980's. The digital commands are then converted to rectifier pulses in firing generators inside the individual rectifier supplies. A block diagram showing the layout of the NSTX control system is shown in Figure 1.

3 Software Infrastructure

The software infrastructure (i.e. the part of the software that performs the human interface, shot restore, data archiving, network functionality, etc.) was largely adopted from the Plasma Control System [8] developed at General Atomics, although adaptations were required for use on NSTX [9]. In particular, the data archiving is now compatible with the MDSplus [10] data archiving system. The real-time functions were optimized for the G4-Altivec based real-time floating processors used on NSTX (see above). Data acquisition functions were customized for compatibility with the FPDP data acquisition system described above, and this functionality has been separated from the PCS. Another important feature of the NSTX implementation of the PCS is that power supply control functions are handled digitally - with individual rectifier firing angles generated within a stand-alone program called the Power Supply Real-Time controller (PSRTC) [11].

4 Control Software

The PCS divides control into various categories which, in general, each correspond to a physically different control concept. The current set of control categories on NSTX are:

1. Toroidal Field
2. Plasma current/transformer control
3. Discharge Shape
4. Equilibrium
5. Isoflux
6. System
7. Data Acquisition
8. Gas Injection
9. Error Fields and Resistive Wall Modes

Categories 3 through 6 correspond to plasma shape control. The Discharge Shape category contains a rudimentary control algorithm which controls the plasma radial and vertical position with preprogrammed control of the other coil currents. A precise description of this algorithm follows in the next section. The Equilibrium category inverts the Grad-Shafranov equation using the rtEFIT code; the resulting equilibrium solution provides input to the isoflux category. The isoflux category uses the errors between the flux at the requested boundary and the real-time calculation of the plasma boundary flux as input to a PID type controller that determines the poloidal field coil voltages. The various isoflux algorithms in use in the isoflux category are described in Reference [4]. The system category is used to choose between the Discharge Shape category and the Isoflux category as a source for the poloidal field coil voltage commands. The System category has been recently upgraded to allow for a continuous hand-off from one category to the other using “fuzzy” logic, which has been beneficial for avoiding jumps in the plasma position and shape at the category transition.

Plasma shape control during a plasma pulse on NSTX is in general divided up into three basic phases: 1. Pre-shot set-up phase, including initial breakdown, 2. plasma control phase, 3. Post-shot ramp-down. Phases 1 and 3 involve ramping the coil currents in a pre-programmed manner, and will not be discussed further in this paper. The plasma control phase in general consists of up to several additional phases that can be selected and configured according to the shot requirements.

4.1 Position and Current Control algorithm (PCC)

The initial phase of plasma control on NSTX consists of a plasma current ramp using the PCC algorithm. The PCC algorithm uses magnetics input from 3 flux loops and 4 magnetic field coils as shown in Figure 2. It should be noted that the location for the outer control sensors is determined by the presence of several large obstructions on the outboard mid-plane of NSTX. The radial position measurement is constructed according to the following relations:

$$\Delta\psi_r = \left[\psi_1 + \Delta_{in}\left(\frac{\partial\psi}{\partial R}\bigg|_{1u} + \frac{\partial\psi}{\partial R}\bigg|_{1l}\right)\right] - \left[(\psi_2 + \psi_3)/2 + \Delta_{out}\left(\frac{\partial\psi}{\partial R}\bigg|_{2} + \frac{\partial\psi}{\partial R}\bigg|_{3}\right)/2\right]$$

where $\frac{\partial\psi}{\partial R}\big|_i = 2\pi R_i B_{v_i}$ and B_{v_i} is the measured vertical magnetic field at the ith spatial location $[R_i, Z_i]$, and Δ_{in} and Δ_{out} are the requested inner and outer gaps, respectively. The radial equilibrium is maintained by controlling the current in the PF5 coil (see Figure 2 for PF5 coil location). The PF5 coil voltage is set to:

$$V_{PF5} = G_{P_r}\Delta\psi_r + G_{I_r}\int_0^t \Delta\psi_r dt + G_{D_r}\frac{d\Delta\psi_r}{dt}$$

This type of control is typically referred to as gap control with a PID (Proportional, Integral, Derivative) algorithm. Vertical position control is based on the flux difference at the outer wall without projecting the flux across the gaps.

$$\Delta\psi_v = (\psi_3 - \psi_2) + \Delta_z I_p \frac{dM_{pv}}{dz}$$

where Δ_z is the requested vertical offset, I_p is the plasma current, and $\frac{dM_{pv}}{dz}$ is the change in the mutual inductance between the plasma and the pair of flux loops used for the vertical position measurement due to a vertical displacement of the plasma. The voltage request to the power supplies is then:

$$\Delta V^j_{PF3} = (-1)^j \left(G_{P_v} \Delta\psi_v + G_{I_v} \int_0^t \Delta\psi_v dt + G_{D_v} \frac{d\Delta\psi_v}{dt} \right) \equiv (-1)^j PID(\Delta\psi_v)$$

Where we have defined the PID operator, and the superscript $j = 0, 1$ refers to [upper,lower] PF3 coils. This voltage offset is then added to the preprogrammed average PF3 current request. The remaining poloidal field coils are preprogrammed, with PID feedback on the coil current error.

4.2 rtEFIT reconstructions

The implementation of the input data for rtEFIT on NSTX exactly mimics the one used for NSTX implementation [12] of the between shots EFIT analysis [13]. A unique feature of the NSTX EFIT implementation is the inclusion of a novel measurement of the vacuum vessel eddy current distribution using loop voltages [14]. This feature has, for the first time, been incorporated into the rtEFIT implementation, allowing for more precise control during plasma current ramps. A comparison of the results of rtEFIT reconstructions and those obtained using the normal between shots analysis can be seen in Figure 3. In general the agreement between the two calculations is quite good but, as can be seen in the figure, differences do exist. The cause of the boundary differences is not due to dissimilarities between the numerical algorithms, but rather to the variations between the input model parameters used in real-time and those used for between shots analysis. In particular, the differences are: 1) Grid resolution (33x33 real time, 65x65 between shots) 2) parameterization of the current profile (fewer parameters are used in real-time due to the stringent convergence requirements) 3) The coil currents and some of the vessel currents are treated as known values rather than as unknowns - also due to time constraints imposed by real-time requirements. The impact of these differences are roughly equally important in determining the differences between the rtEFIT and the offline EFIT boundaries. Faster processors will help to relieve these differences after planned upgrades. Precise position control has been possible in spite of these systematic errors, since they are systematic and reasonably predictable.

The time between iterations of the Grad-Shafranov equation in rtEFIT (referred to as the "slow-loop") using the NSTX control computer is presently 12ms. This time delay is too long for control purposes. In order to deal with faster transients and maximize the bandwidth of the control system, a second routine is used to actually calculate the boundary flux in the control loop. A second calculation, referred to as the "fast-loop" does a least-squares fit of the current to the most recent real-time data, using the most recent rtEFIT flux grid as a constraint. It is this fast loop that actually generates the boundary flux used in the isoflux control, which completes every $400\mu s$ on the NSTX control computer. A more detailed description of the "fast-loop" is presented in Reference [4].

4.3 Isoflux control

The isoflux control algorithm takes advantage of the fact that the plasma boundary is a surface of constant magnetic flux, converting the position control of the 2-D plasma boundary into scalar control of the flux on the boundary. The isoflux algorithms are flexibly configurable - a feature which has allowed the algorithm to be adapted with relative ease to a substantially different magnetic geometry. A typical NSTX isoflux control configuration is shown in Figure 4. The lines in the plot are referred to as control segments. Control points are determined by the intersection of the line segments with the requested plasma boundary. The flux is calculated at this control point in the rtEFIT algorithm. This control flux is then compared to the flux at a predetermined reference point, usually either the flux at (one of) the x-point(s) for a boundary defined by a separatrix or, in the case of a limited discharge, the flux at the limiter. The differences between the reference and control fluxes are then used as the inputs to the isoflux control. In general, each coil voltage is then a linear sum of a PID operator applied to all the control segments, with independent gains for each control point. In practice, to date, the various coils are assigned to control points on a one-to-one basis (i.e. a diagonal gain matrix). X-points are assumed to be inside a control region (also shown in Figure 4) for which the field and flux Green's functions are pre-calculated on a denser grid. The location of each X-point is found iteratively on each time step. If the X-point is located outside this region, the code extrapolates using gradients. The R and Z location of the X-point can be controlled independently - therefore requiring (at least) 2 coils to adequately control the location of the X-point.

NSTX presents a unique control challenge relative to other tokamaks, in that there are no coils on the inboard radius of the plasma. This complicates control of the inner gap in divertor discharges. In particular, it is not possible to independently control the inner gap and each point on the outer boundary. The problem is further complicated by the small number of poloidal field coils on the outboard major radius side of the plasma. For example, a scan of plasma triangularity at fixed elongation and aspect ratio made using a predictive equilibrium solver is shown in Figure 5. As is apparent in the figure, the upper and lower outer squareness of the discharges must change in order to maintain the other specified shape moments (ϵ, κ, δ corresponding to inverse aspect ratio, elongation, triangularity). The solution currently in use on NSTX to address this problem is to vary the outer squareness manually in order to achieve the requested inner gap. The problems associated with the limitations imposed by the ST geometry and limited PF coil set have not prevented the achievement of precision control - a promising result for future ST devices.

4.4 Control transition

The control transition between the PCC algorithm and the rtEFIT algorithm has been implemented using "fuzzy" logic. A programmable waveform $W(t)$ is defined and allowed to vary between 0 and 1. Typically, the transition is programmed as a linear ramp over a period of $\sim 40ms$ from the PCC algorithm to the rtEFIT/isoflux control. The actual voltage request is therefore given by:

$$V_i = \big(1 - W(t)\big) V_{PCC_i} + W(t) * V_{isoflux_i}$$

where the subscript i indexes the poloidal field coil in question.

5 Control examples

The rtEFIT/isoflux control system was initially commissioned in July 2002 and was also used in a few shots during the brief 2003 physics campaign. In 2004 rtEFIT/isoflux was used as an effective operational tool, with 40% of plasma discharges using this system for control. Control with rtEFIT/isoflux was demonstrably better in many regards, enabling several experiments that would have otherwise been much more time consuming, if not impossible.

In Figure 6 the plasma boundaries as reconstructed by EFIT from four double null divertor plasma discharges are overlaid. The EFIT reconstructions were performed on a 1ms time grid through the 300ms plasma current flattop in each discharge for a total of 1200 reconstructions. As can be seen from the plot, the boundary control and the shot-to-shot reproducibility are quite good. The remaining small changes in the boundary relative to the request are caused by leakage flux from the transformer causing the X-points to drift towards the mid-plane slightly as the shot progresses. This remaining drift will be either explicitly compensated, or a larger X-point integral term will be added to compensate for this motion. A detailed view of the quality of the control is shown in Figure 7, which shows the difference between the requested location of the outboard mid-plane radius and that reconstructed by EFIT and rtEFIT. There is a 1.3cm shift between the requested plasma boundary and that reconstructed by rtEFIT, caused by the finite gain of the feedback system (the integral gain is small for the outer gap). There is an additional systematic shift between the rtEFIT reconstruction and the EFIT reconstruction caused by the differing inputs, as noted above. The RMS fluctuating error is 3.3mm, which is mostly due to plasma motions caused by sawteeth.

The rtEFIT/isoflux control scheme has also been used to dynamically control boundary changes during a single plasma shot. Three reconstructed equilibria are shown in Figure 8 from a single shot in which the parameter δr_{sep} is requested to vary linearly in time, where δr_{sep} is defined as the radial distance measured at the outboard midplane between the flux surfaces upon which the upper and lower x-points lie. The variation is achieved by adding a voltage either to the PF3U coil or the PF3L coil as determined by a PID operation on the error between the flux difference at the 2 x-points and the flux difference between the outboard midplane control point and a point that is shifted by the requested δr_{sep} away. This flux error can be expressed as:

$$\Delta\psi_{\delta r_{sep}} = \big(\psi_{x1} - \psi_{x2}\big) - \big(\psi(R_0 + a + \delta r_{sep}) - \psi(R_0 + a)\big)$$

In addition, in order to keep the control points corresponding to PF3 consistent with the the now deformed plasma boundary, the positions of the PF3 control point is shifted by an amount given by:

$$\Delta_{PF3} = C * \delta r_{sep}$$

Where C is programmable factor adjusted to correspond to the flux expansion between the midplane and the control point.

Shown in Figure 9 is δr_{sep} as calculated by EFIT for a series of consecutive discharges for which the δr_{sep} parameter was systematically varied. Also shown in the figure is the time history of the innermost, central and outermost major radius of the discharge, along with the top, vertical centroid, and bottom of the plasma. As can be seen from the figure, the major radius was held fixed as the X-point configuration was varied over a wide range. Fixing the outer gap is important, since coupling of RF heating power to the plasma depends sensitively on the position of the plasma relative to the RF antenna. The radio frequency power was coupled to the plasma efficiently in each of the cases shown. The availability of the boundary flux in real-time facilitates precise shot-to shot variation with accurate control of boundary parameters.

6 Summary

The rtEFIT/isoflux control algorithm has been used for plasma control on the National Spherical Torus Experiment, the first time such advanced control techniques have been applied to a spherical tokamak. As expected, control based on accurate plasma reconstructions has provided improved flexibility and accuracy in experimental operations. For the first time on any device, the measured eddy currents were used in the real-time reconstruction, enabling more accurate reconstruction of the plasma boundary. This was possible in spite of the limitations imposed by the absence of poloidal field coils on the inboard major radius side of the plasma. A "fuzzy logic" control scheme has been applied that has smoothed the transition between the initial plasma control and the isoflux/rtEFIT control, making these transitions more reliable. Planned upgrades to faster processors should improve the control further.

This work was supported by the U.S. Department of Energy Grant under contract number DE-AC02-76CH03073. The authors would like to dedicate this work to the memory of Tom Gibney, whose work made this effort possible.

References

[1] J. Hugill and A. Gibson, Nucl. Fusion **14** 611 (1974)

[2] H. Grad and H. Rubin, in proceedings of the Second United Nations International Conference on the Technology of Fusion Energy, San Francisco, California, p. 19 (1958)

[3] V. D. Shafranov, Sov. Phys. JETP **26**, 682 (1960)

[4] J. R. Ferron, M. L. Walker, L. L. Lao, et al., Nucl. Fusion **38** 1055 (1998)

[5] F. Hoffman and S. C. Jardin, Nucl. Fusion **30** 2013 (1990)

[6] J. R. Wilson, R. E. Bell, S. Bernabei, et al., Phys. Plasmas **10** Part 2 1733 (2003)

[7] R. Raman, T. R. Jarboe, D. Mueller, et al., Plasma Phys. Cont. Fusion. **43** 305 (2001)

[8] B. G. Penaflor, D. A. Piglowski, J. R. Ferron, M. L. Walker, IEEE Trans. Nucl. Science **47** 201 (2000)

[9] D. Mastrovito, J. Ferron, D. Gates, T. Gibney, R. Johnson, Fus. Eng. and Design **71** 65 (2004)

[10] J. A. Stillerman, T. W. Fredian, K. A. Klare, G. Manduchi, Rev. Sci. Inst. **68** 939 (1997)

[11] C. Neumeyer, P. Heitzenroeder, J. Spitzer, et al., Fusion Eng. and Design, **54** 275 (2001)

[12] S. A. Sabbagh, R. E. Bell, M. G. Bell, et al., Nucl. Fusion **41** 1601 (2001)

[13] L. L. Lao, H. St. John, R. D. Stambaugh, et al., Nucl. Fusion **25** 1421 (1985)

[14] D. A. Gates, J. E. Menard, and R. J. Marsala, Rev. Sci. Inst. **75** 5090 (2004)

Figure Captions

Figure 1: Block diagram showing the layout of the NSTX control system.

Figure 2: Figure showing the location of the magnetic sensors in use for rtEFIT/isoflux control. Green circles indicate the location of flux loops, while blue circles indicate magnetic field sensors. Red circles indicate flux loops that are also used as voltage loops for determining the vessel eddy current distribution. The vessel is color coded according to material resistivity as in Reference [14]. Also indicated are the locations of the sensors used for the position and current control (PCC) algorithm.

Figure 3: Figure comparing the plasma boundary as determined by EFIT (solid line) and rtEFIT (dashed line).

Figure 4: Figure showing the control segments (black lines) and control points (green circles) used in the rtEFIT/isoflux control scheme. The shaded red boxes are the regions in which an X-point is assumed to be located. The plasma boundary in the figure is a typical elongated NSTX double null boundary.

Figure 5: Scan of triangularity for a series of discharges with fixed elongation and aspect ratio, showing the squareness changes to preserve the other shape moments.

Figure 6: 1200 reconstructed plasma boundaries calculated at 1ms intervals for 4 plasma discharges showing excellent control of the plasma boundary with rEFIT/isoflux.

Figure 7: Error between EFIT and rtEFIT as a function of time for shot 114184, one of the shots in Figure 6 (dashed line) and also between EFIT and the radius of the control request (solid line). The RMS deviation of the EFIT boundary from the requested radius is 3.3mm with a fixed offset of 2.4cm, 1.3cm of which is due to the difference between EFIT and rtEFIT.

Figure 8: A series of 3 equilibria at different times during a discharge for which the parameter δr_{sep} was programmed to vary linearly from +2 cm to -2cm during the discharge. The blue points are the control points. The green points are the actual positions of the X-points, the heights of which are controlled to be fixed.

Figure 9: Time history of 13 shots for which the parameter δr_{sep} was systematically varied from -2cm to +2cm. Shown in sequence are a) plasma current in MA, b) δr_{sep} in centimeters, c) inboard major radius, radial geometric center, and outboard major radius of the discharge, and d) top, vertical geometric center, and bottom of the plasma.

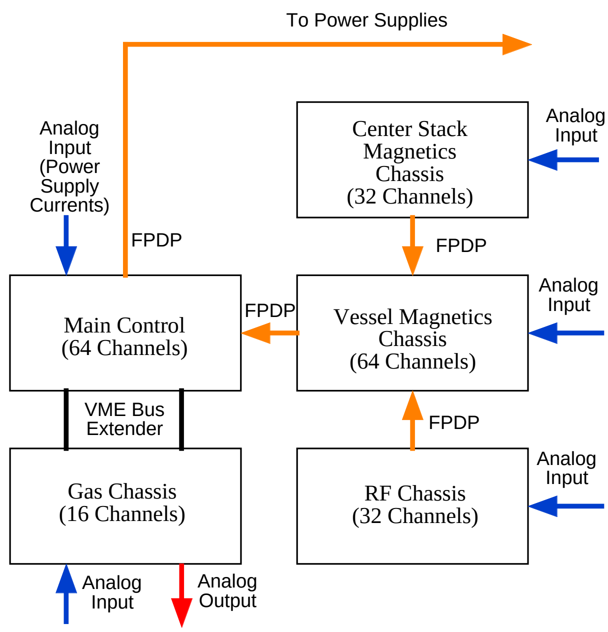
To Power Supplies
Analog Input (Power Supply Currents)
FPDP
Center Stack Magnetics Chassis (32 Channels)
Analog Input
FPDP
Main Control (64 Channels)
FPDP
Vessel Magnetics Chassis (64 Channels)
Analog Input
VME Bus Extender
FPDP
Gas Chassis (16 Channels)
RF Chassis (32 Channels)
Analog Input
Analog Input
Analog Output

Figure 1:

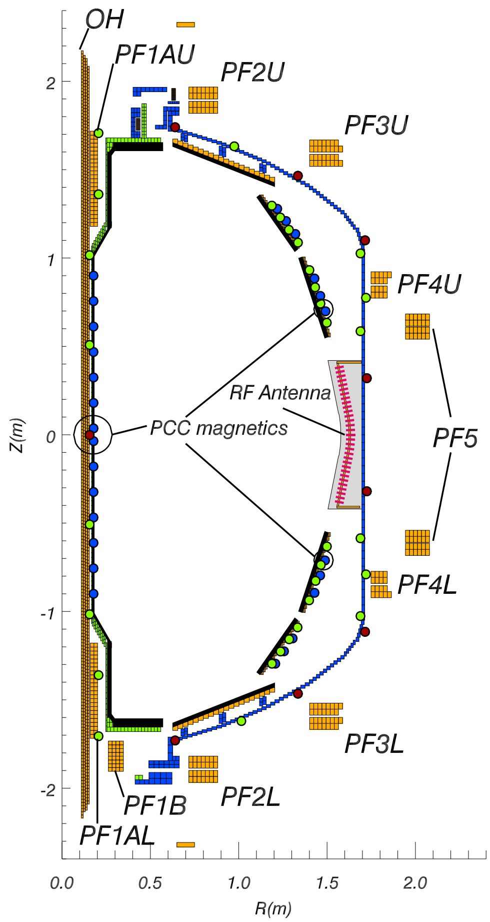
OH
PF1AU
PF2U
PF3U
PF4U
PF5
RF Antenna
PCC magnetics
PF4L
PF3L
PF2L
PF1B
PF1AL
Z(m)
R(m)
2
1
0
-1
-2
0.0
0.5
1.0
1.5
2.0

Figure 2:

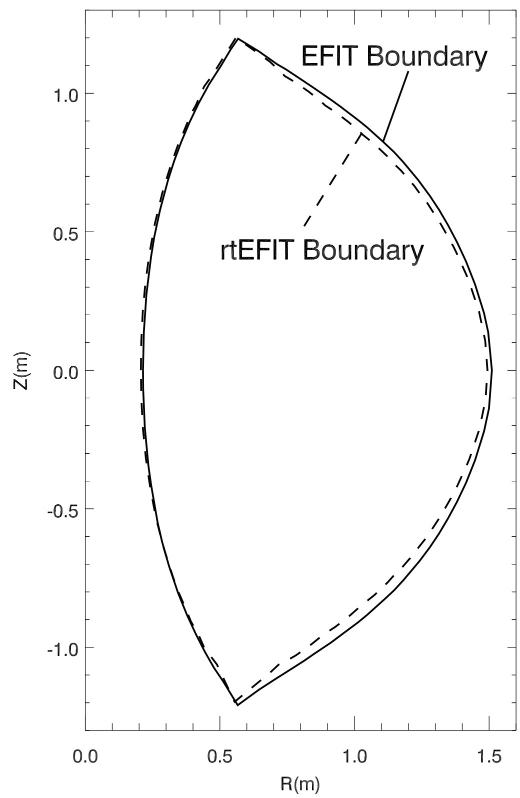

Figure 3:

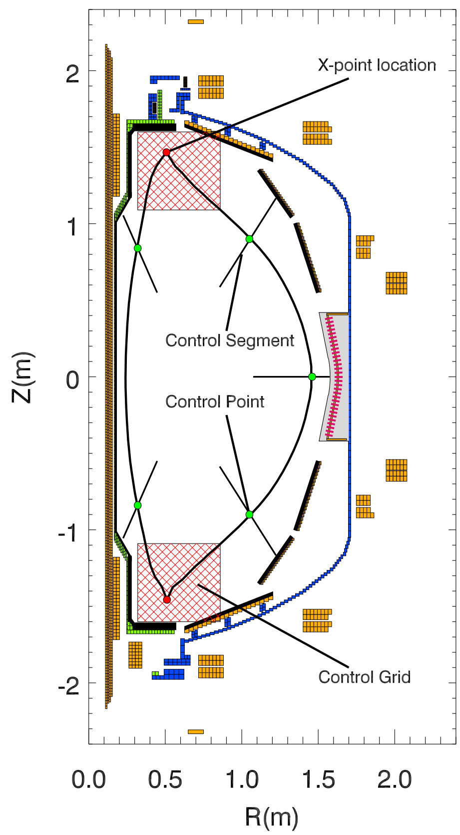
X-point location
Control Segment
Control Point
Control Grid
Z(m)
R(m)
2
1
0
-1
-2
0.0
0.5
1.0
1.5
2.0

Figure 4:

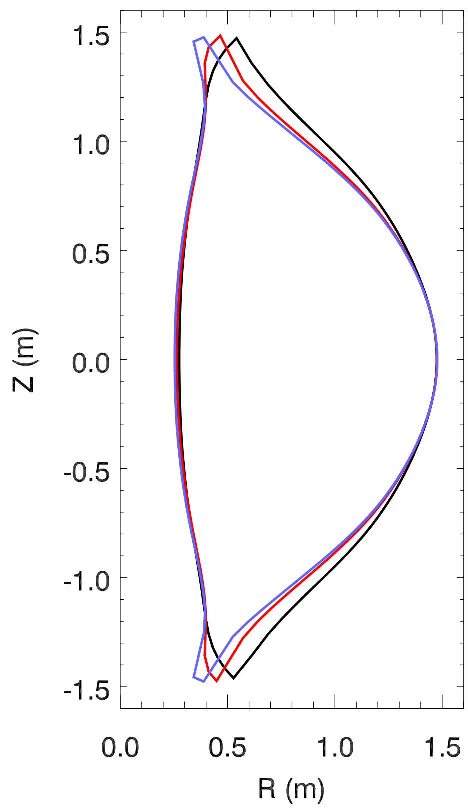

Figure 5:

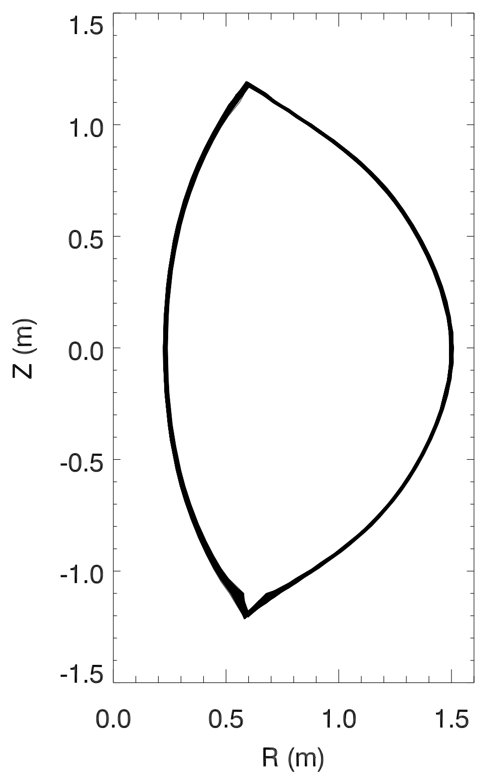

Figure 6:

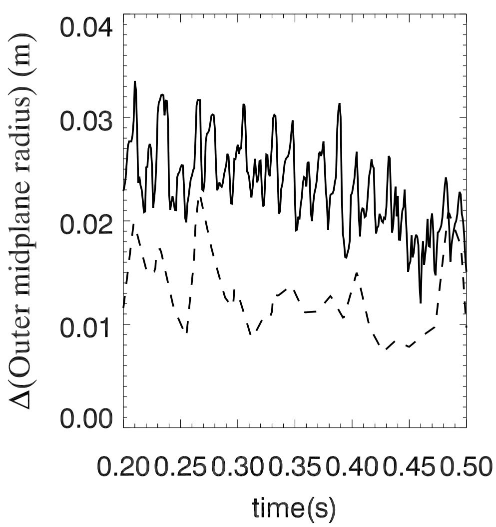
0.04
0.03
0.02
0.01
0.00
Δ(Outer midplane radius) (m)
0.20
0.25
0.30
0.35
0.40
0.45
0.50
time(s)

Figure 7:

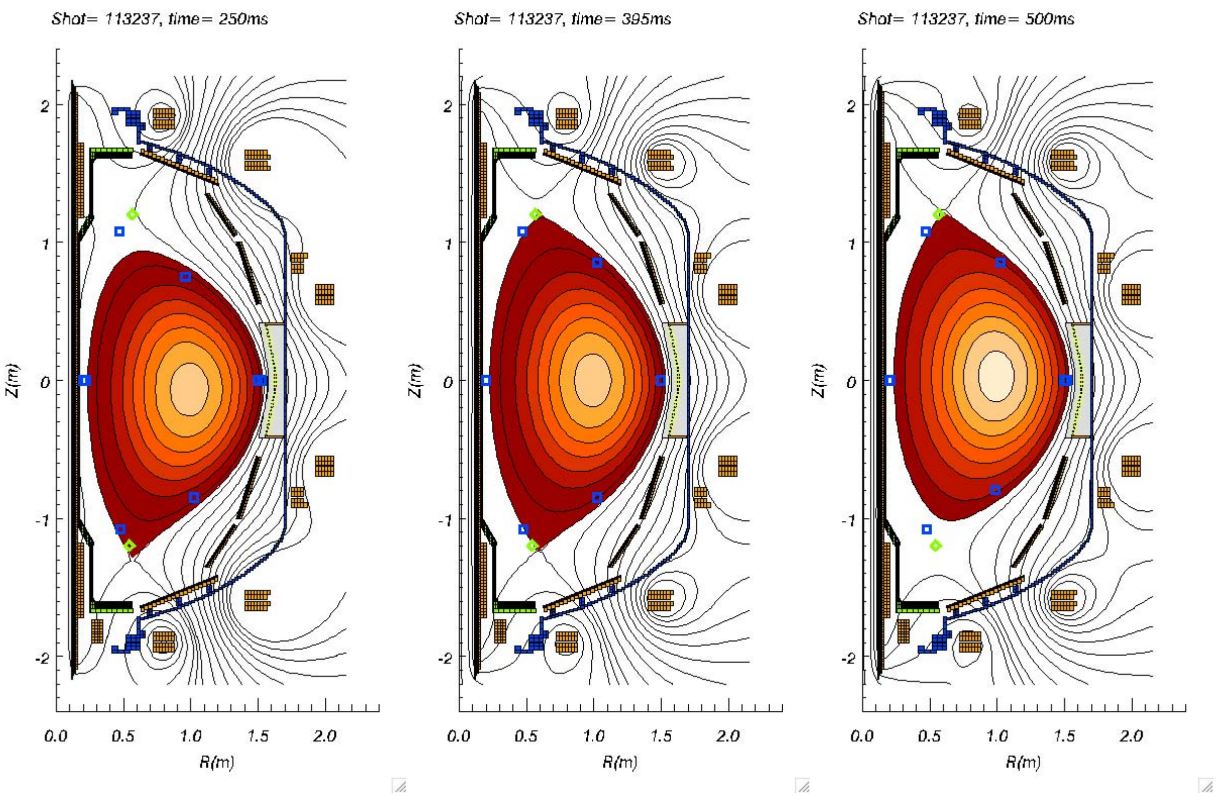

Shot= 113237, time= 250ms
Shot= 113237, time= 395ms
Shot= 113237, time= 500ms
Z(m)
R(m)

Figure 8:

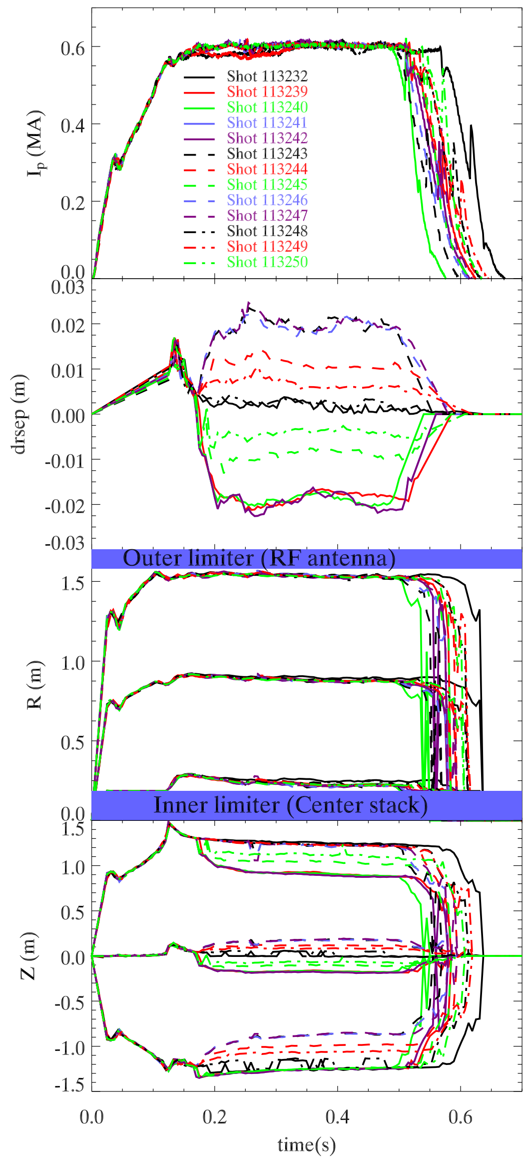

Shot 113232
Shot 113239
Shot 113240
Shot 113241
Shot 113242
Shot 113243
Shot 113244
Shot 113245
Shot 113246
Shot 113247
Shot 113248
Shot 113249
Shot 113250
Ip (MA)
drsep (m)
Outer limiter (RF antenna)
R (m)
Inner limiter (Center stack)
Z (m)
time(s)

Figure 9:

External Distribution

Plasma Research Laboratory, Australian National University, Australia
Professor I.R. Jones, Flinders University, Australia
Professor João Canalle, Instituto de Fisica DEQ/IF - UERJ, Brazil
Mr. Gerson O. Ludwig, Instituto Nacional de Pesquisas, Brazil
Dr. P.H. Sakanaka, Instituto Fisica, Brazil
The Librarian, Culham Science Center, England
Mrs. S.A. Hutchinson, JET Library, England
Professor M.N. Bussac, Ecole Polytechnique, France
Librarian, Max-Planck-Institut für Plasmaphysik, Germany
Jolan Moldvai, Reports Library, Hungarian Academy of Sciences, Central Research Institute for Physics, Hungary
Dr. P. Kaw, Institute for Plasma Research, India
Ms. P.J. Pathak, Librarian, Institute for Plasma Research, India
Dr. Pandji Triadyaksa, Fakultas MIPA Universitas Diponegoro, Indonesia
Professor Sami Cuperman, Plasma Physics Group, Tel Aviv University, Israel
Ms. Clelia De Palo, Associazione EURATOM-ENEA, Italy
Dr. G. Grosso, Instituto di Fisica del Plasma, Italy
Librarian, Naka Fusion Research Establishment, JAERI, Japan
Library, Laboratory for Complex Energy Processes, Institute for Advanced Study, Kyoto University, Japan
Research Information Center, National Institute for Fusion Science, Japan
Dr. O. Mitarai, Kyushu Tokai University, Japan
Dr. Jiangang Li, Institute of Plasma Physics, Chinese Academy of Sciences, People's Republic of China
Professor Yuping Huo, School of Physical Science and Technology, People's Republic of China
Library, Academia Sinica, Institute of Plasma Physics, People's Republic of China
Librarian, Institute of Physics, Chinese Academy of Sciences, People's Republic of China
Dr. S. Mirnov, TRINITI, Troitsk, Russian Federation, Russia
Dr. V.S. Strelkov, Kurchatov Institute, Russian Federation, Russia
Professor Peter Lukac, Katedra Fyziky Plazmy MFF UK, Mlynska dolina F-2, Komenskeho Univerzita, SK-842 15 Bratislava, Slovakia
Dr. G.S. Lee, Korea Basic Science Institute, South Korea
Dr. Rasulkhozha S. Sharafiddinov, Theoretical Physics Division, Insitute of Nuclear Physics, Uzbekistan
Institute for Plasma Research, University of Maryland, USA
Librarian, Fusion Energy Division, Oak Ridge National Laboratory, USA
Librarian, Institute of Fusion Studies, University of Texas, USA
Librarian, Magnetic Fusion Program, Lawrence Livermore National Laboratory, USA
Library, General Atomics, USA
Plasma Physics Group, Fusion Energy Research Program, University of California at San Diego, USA
Plasma Physics Library, Columbia University, USA
Alkesh Punjabi, Center for Fusion Research and Training, Hampton University, USA
Dr. W.M. Stacey, Fusion Research Center, Georgia Institute of Technology, USA
Dr. John Willis, U.S. Department of Energy, Office of Fusion Energy Sciences, USA
Mr. Paul H. Wright, Indianapolis, Indiana, USA

03/07/05

The Princeton Plasma Physics Laboratory is operated
by Princeton University under contract
with the U.S. Department of Energy.

Information Services
Princeton Plasma Physics Laboratory
P.O. Box 451
Princeton, NJ 08543

Phone: 609-243-2750
Fax: 609-243-2751
e-mail: pppl_info@pppl.gov
Internet Address: http://www.pppl.gov